Available online at www.sciencedirect.com
ScienceDirect
Journal of Sound and Vibration 312 (2008) 166–181
JOURNAL OF SOUND AND VIBRATION
www.elsevier.com/locate/jsvi

Free and forced vibration of cracked inhomogeneous beams under an axial force and a moving load

J. Yang[a,*], Y. Chen[a,b], Y. Xiang[c], X.L. Jia[a]

[a]*Department of Building and Construction, City University of Hong Kong, Tat Chee Avenue, Kowloon, Hong Kong*
[b]*School of Civil Engineering, Beijing Jiao Tong University, 100044 Beijing, PR China*
[c]*School of Engineering, University of Western Sydney, Penrith South, NSW 1797, Australia*

Received 19 June 2007; received in revised form 13 October 2007; accepted 20 October 2007
Available online 26 November 2007

Abstract

This paper presents an analytical study on the free and forced vibration of inhomogeneous Euler–Bernoulli beams containing open edge cracks. The beam is subjected to an axial compressive force and a concentrated transverse load moving along the longitudinal direction. The rotational spring model is used to model the crack causing sectional flexibility. The forced response is determined by employing modal series expansion technique. Analytical solutions of natural frequencies and dynamic deflections are obtained for cantilever, hinged–hinged, and clamped–clamped beams whose material properties follow an exponential through-thickness variation. Numerical results are given in both tabular and graphical forms. The effects of cracks, material property gradient, axial compression, and the speed of the moving load are discussed in detail in the parametric study.
© 2007 Elsevier Ltd. All rights reserved.

1. Introduction

It is known that a structure becomes more flexible and its dynamic characteristics will be changed due to the presence of cracks. Over the last decade, the dynamic behavior of cracked structures has been a topic of active research. Many studies have been conducted, either analytically or numerically or both, on the ''direct problem'' and ''inverse problem'' of cracked structures [1–8]. The direct problem involves the determination of natural frequencies and dynamic response of a cracked structure with knowing crack parameters, providing information that is essential to the inverse problem which deals with detecting, locating, and quantifying the extent of damage from the knowledge of measured vibratory data.

When subjected to a moving load or mass, a beam structure produces larger deflections and higher stresses than it does under an equivalent load applied statically. Such a structure is of practical importance, especially in transportation system and in the design of machining process. Quite a few studies have been reported in this field [9–11]. However, research work concerning the effect of cracks on free and forced vibration of a beam under a moving load or mass is still limited. Mahmoud [12] used a modal analysis based approach to calculate

*Corresponding author. Tel.: +852 219 42895; fax: +852 278 87612.
E-mail address: jyang2@cityu.edu.hk (J. Yang).

0022-460X/$ - see front matter © 2007 Elsevier Ltd. All rights reserved.
doi:10.1016/j.jsv.2007.10.034

the stress intensity factor (SIF) of simply supported undamped Euler–Bernoulli beams subjected to a moving load or mass. For the same beams, Mahmoud and Abou Zaid [13] developed an iterative modal analysis method to determine the effect of transverse cracks on the dynamic behavior. Bilello and Bergman [14] carried out a theoretical and experimental study on the response of a damaged Euler–Bernoulli beam traversed by a moving mass. The effective mass distribution of the beam and the convective acceleration terms were considered to correctly evaluate the beam–moving mass interaction force. Lin and Chang [15] obtained an analytical solution of the forced response of a cantilever beam with a crack subjected to a concentrated moving load by using the equivalent rotational spring model, transfer matrix method, and modal series expansion technique. The aforementioned studies considered isotropic homogeneous beams only.

Inhomogeneous composites such as functionally graded materials (FGMs) exhibit a smooth and continuous gradient in both compositional profile and material properties and have received increasing attention in both research and engineering communities due to their outstanding properties. The fracture mechanics and the dynamic characteristics of FGM structures have been the two subject areas attracting a lot of research efforts over the past few years. This is evidenced by numerous publications available in the open literature (see, for example, Refs. [16–20] dealing with cracks and fracture problems and Refs. [21–28] studying free vibration and dynamic response, among many others). It is noted that investigations including the effect of crack defects on the dynamic behavior of FGM structures are scarce. Sridhar et al. [28] analyzed wave propagation in FGM beams and layered structures containing embedded horizontal or vertical edge cracks using pseudospectral finite element method. Most recently, Yang and Chen [29] analytically discussed the influence of open edge cracks on the vibration and elastic stability characteristics of an Euler–Bernoulli FGM beam with different boundary conditions.

This paper investigates the free and forced vibration of slender FGM beams with open edge cracks under a combined action of an axial compression and a concentrated transverse moving load. The classical Euler–Bernoulli beam theory, rotational spring model and modal expansion technique are used to obtain the natural frequencies, mode shapes, and dynamic response of cantilever, hinged–hinged, and clamped–clamped FGM beams with single or multiple cracks. A parametric study is conducted to demonstrate the effects of material property gradient, the location and total number of cracks, the axial compressive force, the moving speed of the concentrated load, the slenderness ratio, and boundary condition on the dynamic behavior of cracked FGM beams.

2. The rotational spring model

Consider a functionally graded beam of length L, thickness h, and containing an open edge crack of depth a located at a distance L_1 from the left end which is taken as the origin of the x–z coordinate system as shown in Fig. 1. The shear modulus v, Young's modulus E, and mass density ρ of the beam vary exponentially in the thickness direction according to

$$v(z) = v_0\, e^{\beta z}, \quad E(z) = E_0\, e^{\beta z}, \quad \rho(z) = \rho_0\, e^{\beta z}, \tag{1}$$

where v_0, E_0, and ρ_0 are the shear modulus, Young's modulus, and mass density at the mid-plane ($z = 0$) of the beam. β is a constant defining the material property gradient along the thickness direction, and as a special

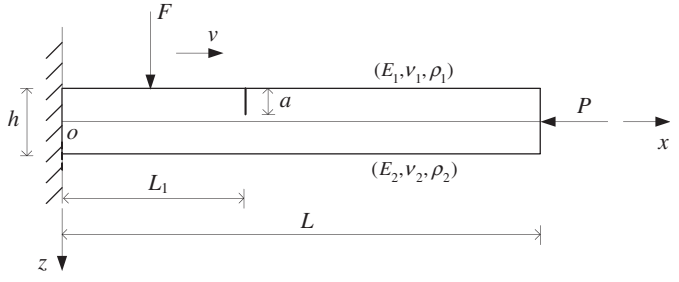

Fig. 1. An axially compressed FGM beam with an open edge crack under a moving load.

case, $\beta = 0$ corresponds to an isotropic homogeneous beam. Since previous study [16] revealed that the influence of Poisson's ratio μ on the SIFs is quite limited, its value is taken as a constant for simplicity in the present analysis.

It is assumed that the crack is perpendicular to the beam surface and always remains open. So the well-accepted rotational spring model can be used to treat the cracked beam as two sub-beams connected by an elastic rotational spring at the cracked section which has no mass and no length. The bending stiffness k_T of the cracked section is related to the flexibility G by

$$k_T = \frac{1}{G}. \tag{2}$$

The flexibility of the beam due to the presence of the edge crack can be calculated from [30]

$$\frac{1-\mu^2}{E(z)} K_I^2 = \frac{M_I^2}{2} \frac{\mathrm{d}G}{\mathrm{d}a}, \tag{3}$$

where M_I is the bending moment at the cracked section. The SIF under mode I loading K_I is a function of the crack depth, beam geometry, external loading, and the material properties. For an FGM strip with an open edge crack under bending, the expression of SIF was derived by Erdogan and Wu [19] as

$$K_I = -\frac{4\sqrt{a}v(z)}{1+\bar{\mu}} \sum_{i=0}^{\infty} \alpha_i T_i\left(\frac{2z-a}{a}\right), \tag{4}$$

where $\bar{\mu} = (3-4\mu)$ for plane strain problem, T_i is the Chebyshev polynomial of the first kind. The constants α_i are determined by evaluating the boundary integrals using Gaussian quadrature and then solving the resulting functional equation by collocation method.

3. Theoretical formulations

Suppose that the cracked FGM beam is subjected to an axial compressive force P and a concentrated transverse load F moving at a constant speed v from the left end of the beam to the right end. Based on the Kirchhoff–Love hypothesis, the displacement components in the x- and z-axis of an arbitrary point, denoted by $\bar{u}(x,z,t)$ and $\bar{w}(x,z,t)$, respectively, take the form of

$$\bar{u}(x,z,t) = u(x,t) - z\frac{\partial \bar{w}}{\partial x}, \tag{5a}$$

$$\bar{w}(x,z,t) = w(x,t), \tag{5b}$$

where $u(x,t)$ and $w(x,t)$ are the mid-plane longitudinal and transverse displacements, t is time. The axial force N, bending moment M, and transverse shear force Q are related to the normal strain $\varepsilon_0 = \partial u/\partial x$ and flexural curvature $k_x = \partial^2 w/\partial x^2$ by

$$\begin{Bmatrix} N \\ M \end{Bmatrix} = \begin{bmatrix} A_{11} & B_{11} \\ B_{11} & D_{11} \end{bmatrix} \begin{Bmatrix} \varepsilon_0 \\ -k_x \end{Bmatrix}, \quad Q = \frac{\partial M}{\partial x} = B_{11}\frac{\partial \varepsilon_0}{\partial x} - D_{11}\frac{\partial k_x}{\partial x}, \tag{6}$$

where

$$(A_{11}, B_{11}, D_{11}) = \int_{-h/2}^{h/2} \frac{E(z)}{1-\mu^2}(1, z, z^2)\,\mathrm{d}z. \tag{7}$$

The equations of motion for a perfect FGM beam without cracks, with the axial inertia term being neglected and the effects of the axial compressive force and the concentrated transverse moving load being included, can be derived as follows:

$$A_{11}\frac{\partial^2 u}{\partial x^2} - B_{11}\frac{\partial^3 w}{\partial x^3} = 0, \tag{8a}$$

$$d\frac{\partial^4 w}{\partial x^4} + P\frac{\partial^2 w}{\partial x^2} + I_1\frac{\partial^2 w}{\partial t^2} = F\delta(x - vt), \tag{8b}$$

where $\delta(x-vt)$ denotes the Dirac delta distribution, and

$$I_1 = \int_{-h/2}^{h/2} \rho(z)\,\mathrm{d}z, \quad d = D_{11} - \frac{B_{11}^2}{A_{11}}. \tag{9}$$

With the introduction of the following quantities:

$$\tilde{W} = \frac{w}{L}, \quad \tilde{U} = \frac{u}{L}, \quad \xi = \frac{x}{L}, \quad \eta = \frac{z}{h}, \quad \Delta_1 = L_1/L, \quad T = \frac{t}{L^2}\sqrt{\frac{d}{I_1}},$$

$$V = vL^2\sqrt{\frac{I_1}{d}}, \quad \gamma = \frac{B_{11}}{A_{11}L}, \quad p = \frac{PL^2}{d}, \quad f = \frac{FL^2}{d}. \tag{10}$$

Eq. (8) can be rewritten in a dimensionless form as

$$\frac{\partial^2 \tilde{U}}{\partial \xi^2} - \gamma\frac{\partial^3 \tilde{W}}{\partial \xi^3} = 0, \tag{11a}$$

$$\frac{\partial^4 \tilde{W}}{\partial \xi^4} + p\frac{\partial^2 \tilde{W}}{\partial \xi^2} + \frac{\partial^2 \tilde{W}}{\partial T^2} = f\delta(\xi - VT). \tag{11b}$$

Neglecting the dynamic force term $f\delta(\xi-VT)$, expressing the dynamic displacements in harmonic vibration as

$$\tilde{U}(\xi, T) = U(\xi)\,\mathrm{e}^{\mathrm{i}\omega T}, \tag{12a}$$

$$\tilde{W}(\xi, T) = W(\xi)\,\mathrm{e}^{\mathrm{i}\omega T}, \tag{12b}$$

where ω is the natural frequency, and then substituting Eq. (12) into Eq. (11b) leads to the equation governing free vibration behavior of the beams

$$\frac{\mathrm{d}^4 W}{\mathrm{d}\xi^4} + p\frac{\mathrm{d}^2 W}{\mathrm{d}\xi^2} - \omega^2 W = 0. \tag{13}$$

By using the rotational spring, the FGM beam with one open edge crack is divided into two sub-beams connected by the spring at the cracked section. In what follows, subscript $i = 1$ and 2 refer to the left and right sub-beams, respectively. The flexural mode shape function of each segment satisfying Eq. (13) can be written as

$$W_i(\xi) = e_{i1}\,\sin(\alpha\xi) + e_{i2}\,\cos(\alpha\xi) + e_{i3}\,\sinh(\beta\xi) + e_{i4}\,\cosh(\beta\xi). \tag{14}$$

Substitution of Eqs. (12) and (14) into Eq. (11a) gives the axial mode shape function

$$U_i(\xi) = \gamma[e_{i1}\alpha\,\cos(\alpha\xi) - e_{i2}\alpha\,\sin(\alpha\xi) + e_{i3}\beta\,\cosh(\beta\xi) + e_{i4}\beta\,\sinh(\beta\xi)] + g_i\xi + g_{i0}, \tag{15}$$

where

$$\alpha = \sqrt{\frac{p}{2} + \sqrt{\frac{p^2}{4} + \lambda^2 L^3}}, \quad \beta = \sqrt{-\frac{p}{2} + \sqrt{\frac{p^2}{4} + \lambda^2 L^3}}, \quad \lambda = \sqrt{\frac{I_1}{d}}\omega,$$

e_{ij} $(i = 1,2; j = 1,\ldots,4)$, g_i and g_{i0} are constants to be determined from boundary conditions at beam ends and the compatibility requirements at the cracked section. For a cantilever beam, the boundary conditions are

$$U_1 = 0, \quad W_1 = 0, \quad \frac{\mathrm{d}W_1}{\mathrm{d}\xi} = 0 \quad \text{at } \xi = 0, \tag{16a}$$

$$N_2 = 0, \quad M_2 = 0, \quad Q_2 - P\frac{\mathrm{d}W_2}{\mathrm{d}\xi} = 0 \quad \text{at } \xi = 1. \tag{16b}$$

At the cracked section ($\xi = \Delta_1$), the compatibility condition enforces the continuity of the axial displacement, transverse displacement, axial force, bending moment, and shear force across the crack. The discontinuity in the slope is proportional to the bending moment transmitted by the cracked section. Thus, we have

$$U_1 = U_2, \quad W_1 = W_2, \tag{17a}$$

$$N_1 = N_2, \quad M_1 = M_2, \quad Q_1 - P\frac{\mathrm{d}W_1}{\mathrm{d}\xi} = Q_2 - P\frac{\mathrm{d}W_2}{\mathrm{d}\xi}, \tag{17b}$$

$$k_T\frac{\mathrm{d}W_1}{\mathrm{d}\xi} - k_T\frac{\mathrm{d}W_2}{\mathrm{d}\xi} = M_1. \tag{17c}$$

Substituting Eqs. (6), (14), (15) into Eqs. (16) and (17) yields a matrix equation

$$[H(\omega)]\{\varphi\} = \{0\}, \tag{18}$$

where $[H]$ is the matrix nonlinearly dependent on the natural frequency, $\{\varphi\}$ is the vector composed of 12 unknown coefficients g_i, g_{i0} and e_{ij} ($i = 1,2$; $j = 1,\ldots,4$). This equation has a non-trivial solution when its determinant is equal to zero

$$\det[H(\omega)] = \left|H(\omega)\right| = 0. \tag{19}$$

By solving this transcendental equation, the natural frequencies and the associated mode shapes can be obtained. The free vibration problem of cracked FGM beams with other boundary conditions can be solved in the same way. The determinants for cantilever, hinged–hinged, and clamped–clamped beams, denoted by H_{c-f}, H_{h-h}, and H_{c-c}, respectively, are given in Appendix A.

4. Forced responses

The modal expansion technique is employed to determine the forced response of the cracked beam. The dynamic deflection of each sub-beam can be expressed as

$$\tilde{W}_i(\xi, T) = \sum_{k=1}^{n} W_{ik}(\xi)q_k(T), \tag{20}$$

where n is the total number of truncated terms, $q_k(T)$ are the generalized coordinates, and $W_{ik}(\xi)$ ($i = 1,2$) represent the normalized mode shapes of the ith sub-beam

$$W_{ik}(\xi) = e_{i1}^k \sin(\alpha\xi) + e_{i2}^k \cos(\alpha\xi) + e_{i3}^k \sinh(\beta\xi) + e_{i4}^k \cosh(\beta\xi). \tag{21}$$

Substituting Eq. (20) into Eq. (11b), multiplying by $W_{ik}(\xi)$ ($i = 1,2$; $j = 1,\ldots,n$) and integrating over each sub-beam, one has

$$\begin{aligned}
&\int_0^{\Delta_1} \sum_{k=1}^{n} [W_{1k}''''(\xi)q_k(T) + pW_{1k}''(\xi)q_k(T) + W_{1k}(\xi)\ddot{q}_k(T)]W_{1j}(\xi)\,\mathrm{d}\xi \\
&\quad + \int_{\Delta_1}^{1} \sum_{k=1}^{n} [W_{2k}''''(\xi)q_k(T) + pW_{2k}''(\xi)q_k(T) + W_{2k}(\xi)\ddot{q}_k(T)]W_{2j}(\xi)\,\mathrm{d}\xi \\
&\quad = \int_0^{\Delta_1} f\delta(\xi - VT)W_{1j}(\xi)\,\mathrm{d}\xi + \int_{\Delta_1}^{1} f\delta(\xi - VT)W_{2j}(\xi)\,\mathrm{d}\xi,
\end{aligned} \tag{22}$$

where a superscript "′" and a super dot denote differentiation with respect to x and T, respectively. With Eq. (13) in mind, the above equation can be simplified as

$$\sum_{k=1}^{n}[\ddot{q}_k(T)+\omega_k^2 q_k(T)]\left[\int_0^{\Delta_1} W_{1k}(\xi)W_{1j}(\xi)\,\mathrm{d}\xi+\int_{\Delta_1}^{1} W_{2k}(\xi)W_{2j}(\xi)\,\mathrm{d}\xi\right]$$
$$=f\left[\int_0^{\Delta_1}\delta(\xi-VT)W_{1j}(\xi)\,\mathrm{d}\xi+\int_{\Delta_1}^{1}\delta(\xi-VT)W_{2j}(\xi)\,\mathrm{d}\xi\right]. \tag{23}$$

Making use of the orthogonality relationship of the normalized mode shapes, Eq. (23) becomes

$$\ddot{q}_k(T)+\omega_k^2 q_k(T)=Q_k(T)\quad(k=1,2,\ldots,n), \tag{24}$$

where

$$Q_k(T)=\begin{cases} f[e_{11}^k\,\sin(\alpha VT)+e_{12}^k\,\cos(\alpha VT)+e_{13}^k\,\sinh(\beta VT)+e_{14}^k\,\cosh(\beta VT)] & \left(T\leqslant\dfrac{\Delta_1 L}{V}\right),\\ f[e_{21}^k\,\sin(\alpha VT)+e_{22}^k\,\cos(\alpha VT)+e_{23}^k\,\sinh(\beta VT)+e_{24}^k\,\cosh(\beta VT)] & \left(T>\dfrac{\Delta_1 L}{V}\right).\end{cases} \tag{25}$$

If the beam is initially in a stationary state, i.e., with zero-valued initial displacement and velocity, before the concentrated load starts to move from the left end, then

$$q_k(T)=\frac{1}{\omega_k}\int_0^{\tau}\sin\,\omega_k(T-\tau)Q_k(\tau)\,\mathrm{d}\tau$$
$$=\begin{cases} \dfrac{f}{\omega_k}\int_0^{\tau}\sin\,\omega_k(T-\tau)\left[e_{11}^k\,\sin(\alpha V\tau)+e_{12}^k\,\cos(\alpha V\tau)+e_{13}^k\,\sinh(\beta V\tau)+e_{14}^k\,\cosh(\beta V\tau)\right]\mathrm{d}\tau & \left(T\leqslant\dfrac{\Delta_1 L}{V}\right)\\ \dfrac{f}{\omega_k}\Big\{\int_0^{\Delta_1/V}\sin\omega_k(T-\tau)\left[e_{11}^k\,\sin(\alpha V\tau)+e_{12}^k\,\cos(\alpha V\tau)+e_{13}^k\,\sinh(\beta V\tau)+e_{14}^k\,\cosh(\beta V\tau)\right]\mathrm{d}\tau & \\ +\int_{\Delta_1/V}^{\tau}\sin\omega_k(T-\tau)\left[e_{21}^k\,\sin(\alpha V\tau)+e_{22}^k\,\cos(\alpha V\tau)+e_{23}^k\,\sinh(\beta V\tau)+e_{24}^k\,\cosh(\beta V\tau)\right]\mathrm{d}\tau\Big\} & \left(T>\dfrac{\Delta_1 L}{V}\right)\end{cases} \tag{26}$$

The forced responses of FGM cracked beams can then be determined from Eq. (20). It should be pointed out that the above analytical solution method, although presented for a single crack, is valid for FGM beams with multiple cracks as well.

5. Numerical results and discussion

To validate the present analysis, the forced vibration response of a homogeneous cantilever beam with an open edge crack of depth $a/h=0.5$ located at $\Delta_1=0.3$ is first considered. The beam is subjected to a transverse point load moving at different speed. The geometrical and material parameters of the beam are: length $L=580\,\mathrm{mm}$, height $h=12.7\,\mathrm{mm}$, Young's modulus $E=206\,\mathrm{GPa}$, and mass density $\rho=7800\,\mathrm{kg/m^3}$. The critical speed of the beam is $V_0=60.9\,\mathrm{m/s}$. Fig. 2 compares the normalized dynamic tip deflections $FL^3/3D_{11}$ with the analytical results reported by Lin and Chang [15]. Excellent agreement is observed.

We now evaluate the free and forced vibration of FGM beams with material parameters $E_1=70\,\mathrm{GPa}$, $\mu_1=0.33$, $\rho_1=2780\,\mathrm{kg/m^3}$ at the top surface and containing one or more open edge cracks by using the analytical solution method described above. The beam is subjected to a combined action of a static axial force and a concentrated transverse load moving along the beam from the left end to the right end at a constant velocity. Numerical results concerning the free vibration characteristics (natural frequencies and mode shapes) are given in Table 1 and Figs. 3–7 while the forced vibration responses are displayed in Figs. 8–12, respectively. In what follows, it is assumed that the crack depth is $a/h=0.2$ and the magnitude of the transverse moving load is not high so that the cracked section of the beam will not be torn. The beam height is kept constant while the beam length may be varied.

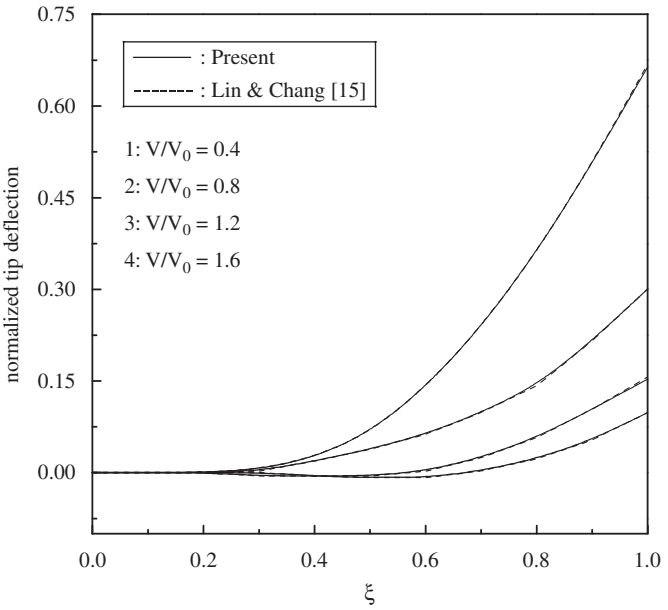

Fig. 2. Dynamic tip deflections of a homogeneous cantilever with an edge crack at $\Delta_1 = 0.3$ under a moving load at different speed.

Table 1
The first three dimensionless natural frequencies of perfect FGM beams

L/h	E_2/E_1	C–F			H–H			C–C		
		$\bar{\omega}_1$	$\bar{\omega}_2$	$\bar{\omega}_3$	$\bar{\omega}_1$	$\bar{\omega}_2$	$\bar{\omega}_3$	$\bar{\omega}_1$	$\bar{\omega}_2$	$\bar{\omega}_3$
20	0.2	0.83	5.18	14.49	2.51	9.27	21.07	5.25	14.49	28.40
	1.0	0.88	5.51	15.42	2.47	9.87	22.21	5.59	15.42	30.23
	5.0	0.83	5.18	14.49	2.51	9.27	21.07	5.25	14.49	28.40
10	0.2	3.30	20.70	57.97	10.05	37.09	84.28	21.02	57.94	113.59
	1.0	3.52	22.03	61.70	9.87	39.48	88.83	22.37	61.67	120.90
	5.0	3.30	20.70	57.97	10.05	37.09	84.28	21.02	57.94	113.59

Table 1 lists the first three dimensionless natural frequencies of cantilever (C–F), hinged–hinged (H–H), and clamped–clamped (C–C) perfect FGM beams with different material property gradients ($E_2/E_1 = 0.2,1.0,5.0$) and slenderness ratios ($L/h = 10,\ 20$), where $E_2/E_1 = 1.0$ corresponds to an isotropic homogeneous beam whose values of d and I_1 are denoted, respectively, by d_0 and I_0 to normalize the frequencies as $\overline{\omega}_n = \omega_n/\sqrt{d_0/I_0}$. It is found that the natural frequencies of FGM beams with $E_2/E_1 = 0.2$ and 5.0 are the same because the ratios of d/I_1 for these two beams are almost identical. The isotropic homogeneous beams, except the hinged–hinged one, have higher dimensionless frequencies than FGM beams.

Fig. 3 shows the fundamental frequency ratio ω_1/ω_{10} of an axially compressed FGM cantilever ($P/P_{cr} = 0.0,0.1,0.3$) with an edge crack at varying locations, where ω_{10} is the fundamental frequency of its perfect counterpart, and P_{cr} is the critical buckling load of the cracked beam that can be calculated using the approach detailed in our previous study [29]. The fundamental frequency ratio is significantly decreased due to the presence of the axial compressive force and the open edge crack. The greater the compressive force is applied, and the closer to the fixed end of the cantilever beam the crack is located, the lower the fundamental frequency becomes. The frequency ratio reaches its lowest value when the crack is at the fixed end. Since the bending stiffness of a FGM beam is lower as Young's modulus ratio E_2/E_1 changes from 5.0 to 0.2, its frequency ratio decreases accordingly, indicating that a weaker beam is more sensitive to the compressive load and crack.

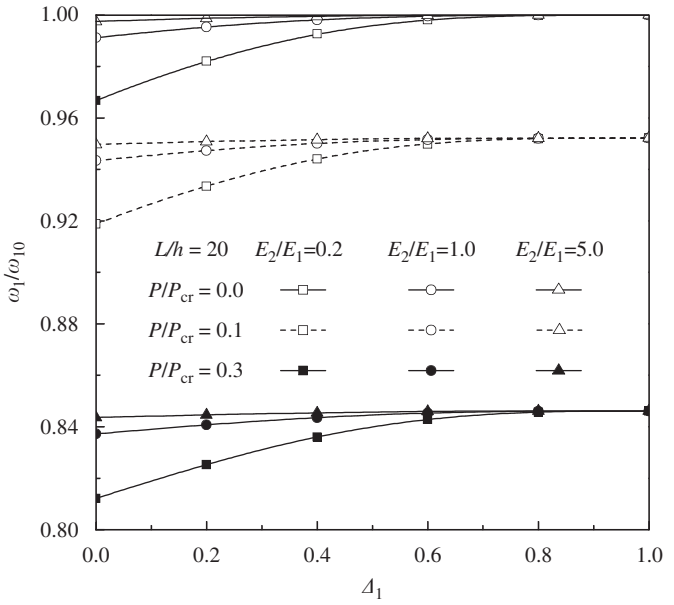

Fig. 3. Fundamental frequency ratio of axially compressed FGM cantilevers with an edge crack at varying locations.

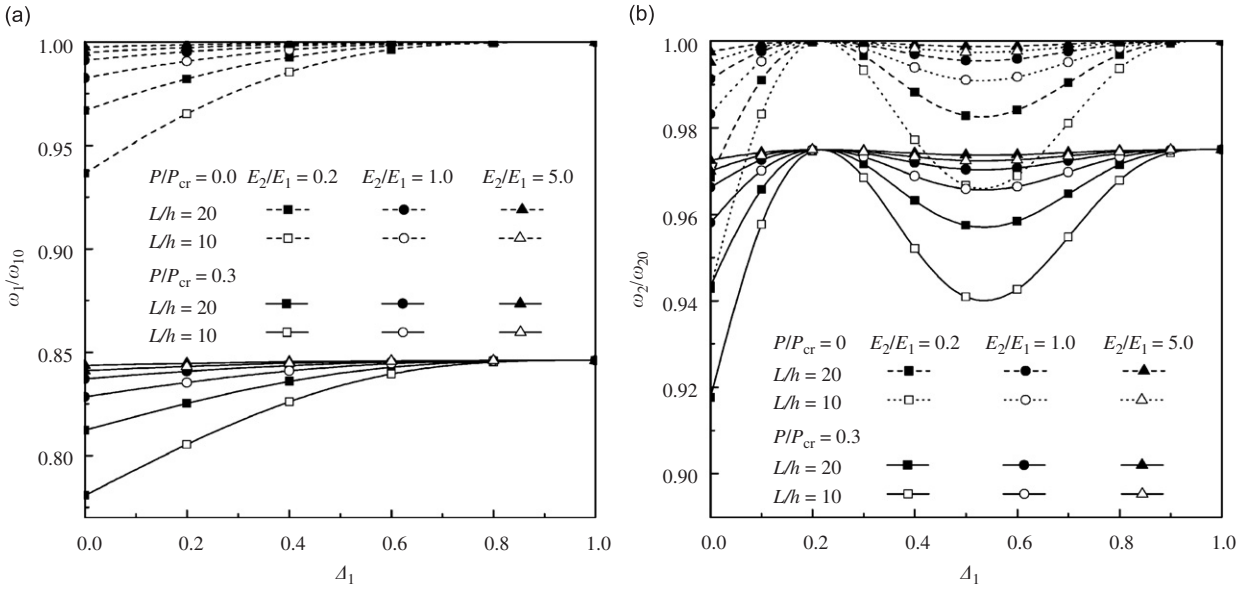

Fig. 4. Effect of slenderness ratio on frequency ratios of axially compressed FGM cantilevers with an edge crack at varying locations: (a) fundamental frequency ratio; and (b) the second frequency ratio.

Fig. 4 depicts the frequency ratio versus crack location curves for the first two frequencies of axially compressed FGM cantilevers ($E_2/E_1 = 0.2,1.0,5.0$, $L/h = 10,20$, $P/P_{cr} = 0.0,0.3$) with a single edge crack. The results for the second frequency are much more complicated than those for the fundamental frequency. The lowest frequency ratios for the first two frequencies are found to be at the same location—the clamped end of the beam. Numerical results also indicate that a beam with a smaller slenderness ratio is much more sensitive to the crack.

Fig. 5 compares the fundamental frequency ratios of axially compressed FGM beams ($E_2/E_1 = 0.2,1.0,5.0$, $L/h = 20$, $P/P_{cr} = 0.3$) with a single edge crack and different end supports. For geometrically symmetric

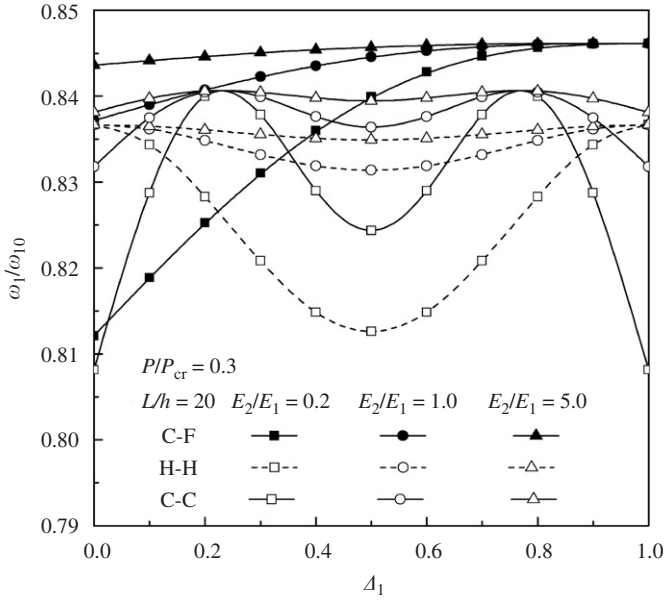

Fig. 5. Fundamental frequency ratio of axially compressed FGM beams with an edge crack and different end supports.

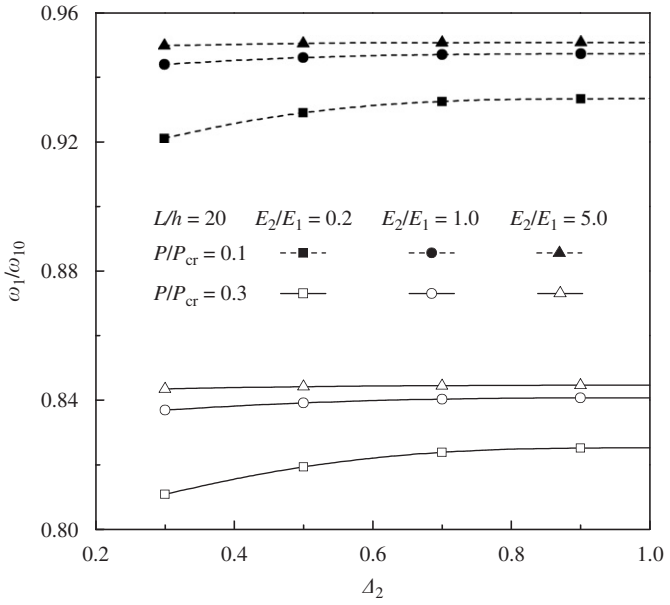

Fig. 6. Fundamental frequency ratio of axially compressed FGM cantilevers with two edge cracks at varying locations ($\Delta_1 = 0.2$).

beams such as the hinged–hinged and clamped–clamped beams, the fundamental frequency ratio versus crack location curves are also symmetric. The fundamental frequency is most affected by the crack when it is located at the mid-point of the hinged–hinged beam or at the clamped ends of the clamped–clamped beam.

Fig. 6 shows the effect of multiple cracks on the fundamental frequency ratio of axially compressed FGM cantilevers ($E_2/E_1 = 0.2$, 1.0, 5.0, $L/h = 20$, $P/P_{cr} = 0.1$, 0.3). It is assumed that the beam contains two edge cracks of the same depth. The first crack is located at $\Delta_1 = 0.2$ while the position of the second crack may be

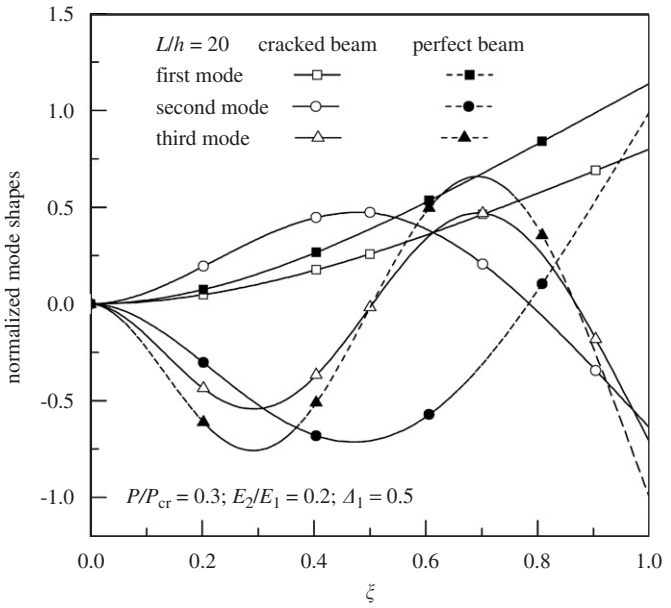

Fig. 7. Vibration mode shapes of axially compressed FGM cantilevers with an edge crack.

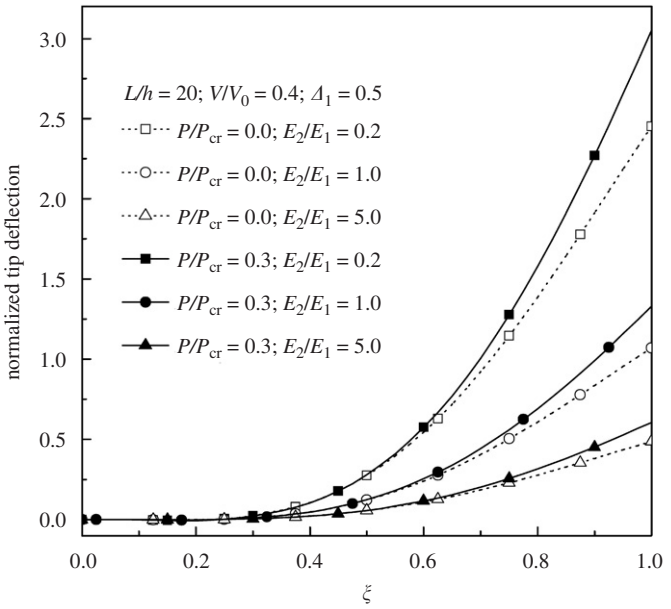

Fig. 8. Dynamic tip deflections of axially compressed FGM cantilevers with an edge crack under a moving load.

varied along the beam length from $\Delta_2 = L_2/L = 0.3$–1.0. The fundamental frequency is slightly lower as the second crack is located closer to the first crack. Compared with the FGM beams with a single edge crack, the beam with two cracks has even lower fundamental frequencies.

Fig. 7 displays the first three mode shapes of axially compressed FGM cantilevers ($E_2/E_1 = 0.2$, $L/h = 20$, $P/P_{cr} = 0.3$) with an edge crack at the mid-point. No mode shape change due to the crack has been observed.

We next investigate the dynamic response of cracked FGM beams under a combined static axial compression and a concentrated transverse load moving along the beam from the left end. Table 2 gives the critical speed, defined as $V_0 = (\lambda_0/L)\sqrt{d/I_1}$ where $\lambda_0^2 = \omega_0\sqrt{I_1/d}$, of cantilever, hinged–hinged, and

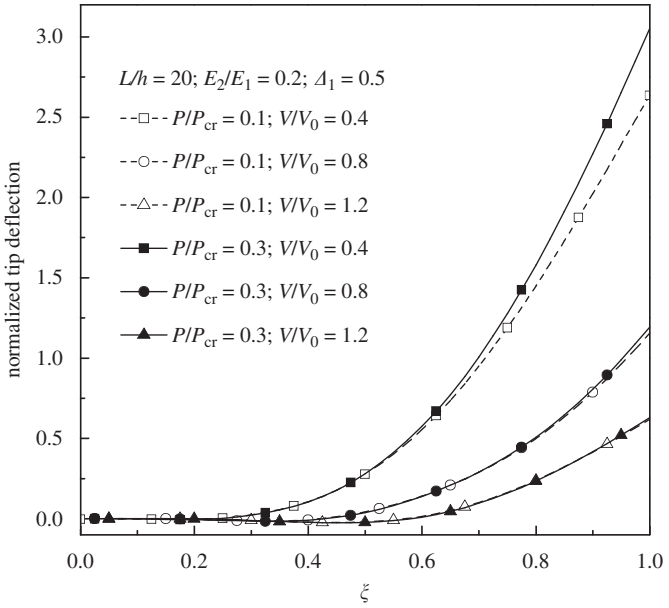

Fig. 9. Dynamic tip deflections of an axially compressed FGM cantilever with an edge crack under different moving load speeds.

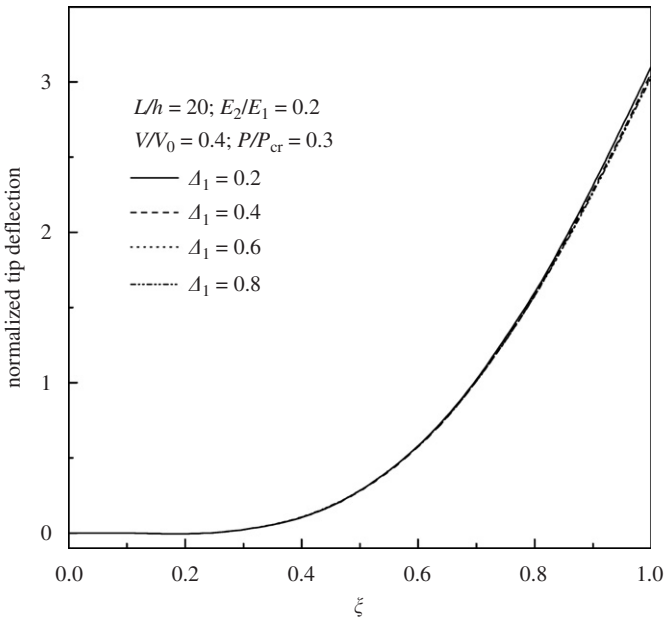

Fig. 10. Dynamic tip deflections of an axially compressed FGM cantilever with an edge crack at different locations.

clamped–clamped perfect FGM beams ($E_2/E_1 = 0.2,\ 1.0,\ 5.0,\ L/h = 20$). The critical speeds of FGM cantilevers with an edge crack at different locations ($\Delta_1 = 0.2, 0.4, 0.6, 0.8$) are listed in Table 3. It is seen that the critical speed of a cracked beam, which is smaller than that of the perfect beam, is only slightly affected by the crack location.

In the following computations, the dynamic deflections in Figs. 8–12 are normalized by the static tip deflection of a perfect homogeneous cantilever under a point load at its free end, i.e., $FL^3/3d_0$. Note that the horizontal axis ξ is the distance the point load has traveled from the left end. Since the moving speed is constant, ξ virtually represents the time the load has traveled. Based on the convergence study we have

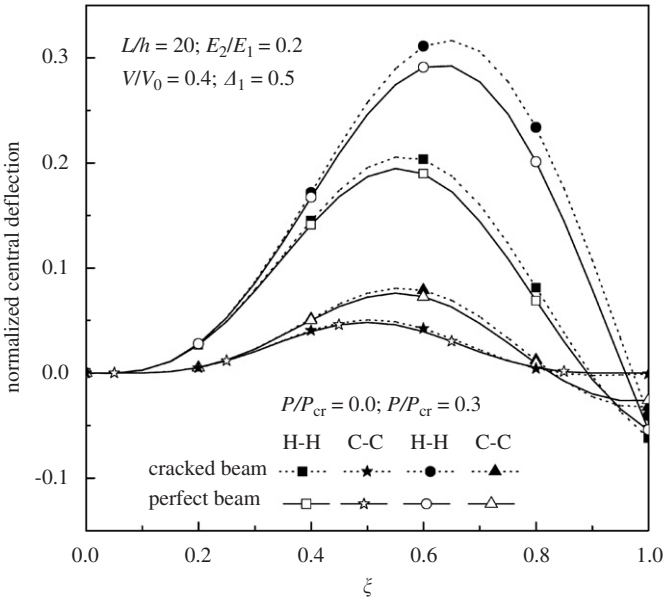

Fig. 11. Dynamic central deflections of axially compressed hinged–hinged and clamped–clamped FGM beams with and without an edge crack under a moving load.

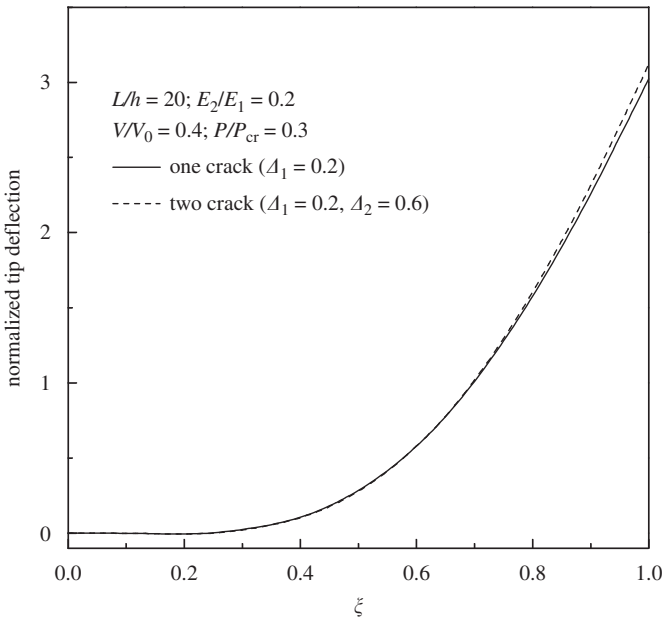

Fig. 12. Dynamic tip deflections of axially compressed FGM cantilevers with one and two edge cracks under a moving load.

conducted but not presented for brevity, the present solution method exhibits excellent convergence characteristics and gives convergent results when the total number of truncated terms in Eq. (20) is $n \geqslant 4$. Hence, $n = 4$ is used in Figs. 8–12.

Fig. 8 demonstrates the effects of both axial compressive force and Young's modulus ratio E_2/E_1 on the dynamic tip deflection of cracked FGM cantilevers ($L/h = 20$, $\Delta_1 = 0.5$) when a point load moves at a speed of $V/V_0 = 0.4$. Figs. 9 and 10 investigate, respectively, how the dynamic tip deflection is influenced by the moving speed of the point load and the crack location. It is observed that the deflection increases with a decrease in Young's modulus ratio and an increase in the axial compression but decreases at a higher value of V/V_0.

Table 2
The critical speed V_0 of perfect FGM beams

L/h	E_2/E_1	V_0 (m/s)		
		C–F	H–H	C–C
20	0.2	135.167	235.775	340.962
	1.0	143.869	241.042	362.914
	5.0	135.167	235.775	340.962

Table 3
The critical speed V_0 of FGM cantilevers with an edge crack

E_2/E_1	$\tilde{V}_0$ (m/s)			
	$\Delta_1 = 0.2$	$\Delta_1 = 0.4$	$\Delta_1 = 0.6$	$\Delta_1 = 0.8$
0.2	122.791	123.588	124.091	124.300
1.0	123.936	124.143	124.273	124.326
5.0	124.222	124.281	124.317	124.332

This is because the beam does not have enough time to reach its maximum deflection when the load moves at a faster speed. The crack location, however, has very little effect on the dynamic tip deflection.

Fig. 11 compares the dynamic deflections at the mid-point of hinged–hinged and clamped–clamped FGM beams ($E_2/E_1 = 0.2$, $L/h = 20$, $V/V_0 = 0.4$) containing an edge crack ($\Delta_1 = 0.5$) with and without an axial compression. As expected, the hinged–hinged beam has much higher deflections than the clamped–clamped beam. The dynamic deflection is much more significantly influenced by the axial compressive load than the edge crack, although both weakening the bending stiffness and consequently resulting in higher bending deformation.

Fig. 12 gives the dynamic tip deflection responses of axially compressed FGM cantilevers ($E_2/E_1 = 0.2$, $L/h = 20$, $V/V_0 = 0.4$, $P/P_{cr} = 0.3$) with one and two edge cracks. The dynamic tip deflection of the cracked beam with two edge cracks is marginally higher than that of the beam with one edge crack.

6. Concluding remarks

Free and forced vibration of FGM Euler–Bernoulli beams with open edge cracks subjected to an axial force and a concentrated moving load is analytically investigated using the rotational spring model and the modal expansion technique. A parametric study has been conducted to examine how the material property gradient, location and the total number of cracks, slenderness ratio, boundary conditions, moving speed of the concentrated load, and the axial compressive force affect the free vibration and dynamic response of the beams. It is found that the natural frequencies decrease and the dynamic deflection increases due to the presence of the edge crack and the axial compressive force. While the natural frequencies are greatly influenced by the edge crack, especially when it is located at some specific positions, the dynamic deflection is not very sensitive to the presence and the location of the edge crack. Both free vibration and dynamic response are much more affected by the axial compression than by the edge crack. The beam with a smaller modulus ratio E_2/E_1 has a lower frequency ratio and higher dynamic deflection.

Acknowledgments

The work described in this paper was fully funded by a research grant from City University of Hong Kong (Project no. 7001958) and a College of Health and Science cross-discipline research grant from University of Western Sydney (Grant no. 20701-71664). The authors are grateful for these financial supports.

Appendix A

In Eq. (19), the determinants for cantilever, hinged–hinged, and clamped–clamped FGM beams with single edge crack are given as below:

$$H_{c-f}=\begin{vmatrix}
0 & 0 & 0 & 0 & 0 & 1 & 0 & 0 & 0 & 0 & 0 & 0\\
0 & 1 & 0 & 1 & 0 & 0 & 0 & 0 & 0 & 0 & 0 & 0\\
\alpha & 0 & \beta & 0 & 0 & 0 & 0 & 0 & 0 & 0 & 0 & 0\\
0 & 0 & 0 & 0 & 0 & 0 & 0 & 0 & 0 & 0 & 1 & 0\\
0 & 0 & 0 & 0 & 0 & 0 & \alpha^2 J_{21} & \alpha^2 J_{22} & -\beta^2 J_{23} & -\beta^2 J_{24} & \frac{B_{11}L}{d_{11}} & 0\\
0 & 0 & 0 & 0 & 0 & 0 & \bar{\alpha} J_{22} & -\bar{\alpha} J_{21} & -\bar{\beta} J_{24} & -\bar{\beta} J_{23} & 0 & 0\\
\frac{B_{11}}{A_{11}L}\alpha J_{12} & -\frac{B_{11}}{A_{11}L}\alpha J_{11} & \frac{B_{11}}{A_{11}L}\beta J_{14} & \frac{B_{11}}{A_{11}L}\beta J_{13} & \Delta_1 & 1 & -\frac{B_{11}}{A_{11}L}\alpha J_{12} & \frac{B_{11}}{A_{11}L}\alpha J_{11} & -\frac{B_{11}}{A_{11}L}\beta J_{14} & -\frac{B_{11}}{A_{11}L}\beta J_{13} & -\Delta_1 & -1\\
J_{11} & J_{12} & J_{13} & J_{14} & 0 & 0 & -J_{11} & -J_{12} & -J_{13} & -J_{14} & 0 & 0\\
0 & 0 & 0 & 0 & 1 & 0 & 0 & 0 & 0 & 0 & -1 & 0\\
-\alpha^2 J_{11} & -\alpha^2 J_{12} & \beta^2 J_{13} & \beta^2 J_{14} & -\frac{B_{11}L}{d_{11}} & 0 & \alpha^2 J_{11} & \alpha^2 J_{12} & -\beta^2 J_{13} & -\beta^2 J_{14} & \frac{B_{11}L}{d_{11}} & 0\\
\bar{\alpha} J_{12} & -\bar{\alpha} J_{11} & -\bar{\beta} J_{14} & -\bar{\beta} J_{13} & 0 & 0 & -\bar{\alpha} J_{12} & \bar{\alpha} J_{11} & \bar{\beta} J_{14} & \bar{\beta} J_{13} & 0 & 0\\
\alpha J_{12}-\frac{d}{Lk_T}\alpha^2 J_{11} & -\alpha J_{11}-\frac{d}{Lk_T}\alpha^2 J_{12} & \beta J_{14}+\frac{d}{Lk_T}\beta^2 J_{13} & \beta J_{13}+\frac{d}{Lk_T}\beta^2 J_{14} & -\frac{B_{11}}{k_T} & 0 & -\alpha J_{12} & \alpha J_{11} & -\beta J_{14} & -\beta J_{13} & 0 & 0
\end{vmatrix}$$

$$H_{c-c}=\begin{vmatrix}
0 & 0 & 0 & 0 & 0 & 1 & 0 & 0 & 0 & 0 & 0 & 0\\
0 & 1 & 0 & 1 & 0 & 0 & 0 & 0 & 0 & 0 & 0 & 0\\
\alpha & 0 & \beta & 0 & 0 & 0 & 0 & 0 & 0 & 0 & 0 & 0\\
0 & 0 & 0 & 0 & 0 & 0 & \frac{B_{11}}{A_{11}L}\alpha J_{22} & -\frac{B_{11}}{A_{11}L}\alpha J_{21} & \frac{B_{11}}{A_{11}L}\beta J_{24} & \frac{B_{11}}{A_{11}L}\beta J_{23} & 1 & 1\\
0 & 0 & 0 & 0 & 0 & 0 & J_{21} & J_{22} & J_{23} & J_{24} & 0 & 0\\
0 & 0 & 0 & 0 & 0 & 0 & \alpha J_{22} & -\alpha J_{21} & \beta J_{24} & \beta J_{23} & 0 & 0\\
\frac{B_{11}}{A_{11}L}\alpha J_{12} & -\frac{B_{11}}{A_{11}L}\alpha J_{11} & \frac{B_{11}}{A_{11}L}\beta J_{14} & \frac{B_{11}}{A_{11}L}\beta J_{13} & \Delta_1 & 1 & -\frac{B_{11}}{A_{11}L}\alpha J_{12} & \frac{B_{11}}{A_{11}L}\alpha J_{11} & -\frac{B_{11}}{A_{11}L}\beta J_{14} & -\frac{B_{11}}{A_{11}L}\beta J_{13} & -\Delta_1 & -1\\
J_{11} & J_{12} & J_{13} & J_{14} & 0 & 0 & -J_{11} & -J_{12} & -J_{13} & -J_{14} & 0 & 0\\
0 & 0 & 0 & 0 & 1 & 0 & 0 & 0 & 0 & 0 & -1 & 0\\
-\alpha^2 J_{11} & -\alpha^2 J_{12} & \beta^2 J_{13} & \beta^2 J_{14} & -\frac{B_{11}L}{d_{11}} & 0 & \alpha^2 J_{11} & \alpha^2 J_{12} & -\beta^2 J_{13} & -\beta^2 J_{14} & \frac{B_{11}L}{d_{11}} & 0\\
\bar{\alpha} J_{12} & -\bar{\alpha} J_{11} & -\bar{\beta} J_{14} & -\bar{\beta} J_{13} & 0 & 0 & -\bar{\alpha} J_{12} & \bar{\alpha} J_{11} & \bar{\beta} J_{14} & \bar{\beta} J_{13} & 0 & 0\\
\alpha J_{12}-\frac{d}{Lk_T}\alpha^2 J_{11} & -\alpha J_{11}-\frac{d}{Lk_T}\alpha^2 J_{12} & \beta J_{14}+\frac{d}{Lk_T}\beta^2 J_{13} & \beta J_{13}+\frac{d}{Lk_T}\beta^2 J_{14} & -\frac{B_{11}}{k_T} & 0 & -\alpha J_{12} & \alpha J_{11} & -\beta J_{14} & -\beta J_{13} & 0 & 0
\end{vmatrix},$$

$$H_{h-h}=\begin{vmatrix}
\frac{B_{11}}{A_{11}L}\alpha & 0 & \frac{B_{11}}{A_{11}L}\beta & 0 & 0 & 1 & 0 & 0 & 0 & 0 & 0 & 0\\
0 & 1 & 0 & 1 & 0 & 0 & 0 & 0 & 0 & 0 & 0 & 0\\
0 & \alpha^2 & 0 & -\beta^2 & \frac{B_{11}L}{d_{11}} & 0 & 0 & 0 & 0 & 0 & 0 & 0\\
0 & 0 & 0 & 0 & 0 & 0 & \frac{B_{11}}{A_{11}L}\alpha J_{22} & -\frac{B_{11}}{A_{11}L}\alpha J_{21} & \frac{B_{11}}{A_{11}L}\beta J_{24} & \frac{B_{11}}{A_{11}L}\beta J_{23} & 1 & 1\\
0 & 0 & 0 & 0 & 0 & 0 & J_{21} & J_{22} & J_{23} & J_{24} & 0 & 0\\
0 & 0 & 0 & 0 & 0 & 0 & \alpha^2 J_{21} & \alpha^2 J_{22} & -\beta^2 J_{23} & -\beta^2 J_{24} & \frac{B_{11}L}{d_{11}} & 0\\
\frac{B_{11}}{A_{11}L}\alpha J_{12} & -\frac{B_{11}}{A_{11}L}\alpha J_{11} & \frac{B_{11}}{A_{11}L}\beta J_{14} & \frac{B_{11}}{A_{11}L}\beta J_{13} & \Delta_1 & 1 & -\frac{B_{11}}{A_{11}L}\alpha J_{12} & \frac{B_{11}}{A_{11}L}\alpha J_{11} & -\frac{B_{11}}{A_{11}L}\beta J_{14} & -\frac{B_{11}}{A_{11}L}\beta J_{13} & -\Delta_1 & -1\\
J_{11} & J_{12} & J_{13} & J_{14} & 0 & 0 & -J_{11} & -J_{12} & -J_{13} & -J_{14} & 0 & 0\\
0 & 0 & 0 & 0 & 1 & 0 & 0 & 0 & 0 & 0 & -1 & 0\\
-\alpha^2 J_{11} & -\alpha^2 J_{12} & \beta^2 J_{13} & \beta^2 J_{14} & -\frac{B_{11}L}{d_{11}} & 0 & \alpha^2 J_{11} & \alpha^2 J_{12} & -\beta^2 J_{13} & -\beta^2 J_{14} & \frac{B_{11}L}{d_{11}} & 0\\
\bar{\alpha}J_{12} & -\bar{\alpha}J_{11} & -\bar{\beta}J_{14} & -\bar{\beta}J_{13} & 0 & 0 & -\bar{\alpha}J_{12} & \bar{\alpha}J_{11} & \bar{\beta}J_{14} & \bar{\beta}J_{13} & 0 & 0\\
\alpha J_{12}-\frac{d}{Lk_T}\alpha^2 J_{11} & -\alpha J_{11}-\frac{d}{Lk_T}\alpha^2 J_{12} & \beta J_{14}+\frac{d}{Lk_T}\beta^2 J_{13} & \beta J_{13}+\frac{d}{Lk_T}\beta^2 J_{14} & -\frac{B_{11}}{k_T} & 0 & -\alpha J_{12} & \alpha J_{11} & -\beta J_{14} & -\beta J_{13} & 0 & 0
\end{vmatrix}$$

in which $J_{11}=\sin(\alpha\Delta_1)$, $J_{12}=\cos(\alpha\Delta_1)$, $J_{13}=\sinh(\beta\Delta_1)$, $J_{14}=\cosh(\beta\Delta_1)$, $J_{21}=\sin(\alpha)$, $J_{22}=\cos(\alpha)$, $J_{23}=\sinh(\beta)$, $J_{24}=\cosh(\beta)$, $\bar{\alpha}=\left(d/L^2\right)\alpha^3-P\alpha$, $\bar{\beta}=\left(d/L^2\right)\beta^3+P\beta$.

References

[1] A.D. Dimarogonas, Vibration of cracked structures: a state of the art review, *Engineering Fracture Mechanics* 55 (1996) 831–857.
[2] G.D. Gounaris, C.A. Papadopuulost, A.D. Dimarogonast, Crack identification in beams by coupled response measurements, *Computers & Structures* 58 (1996) 299–305.
[3] K. El Bikri, R. Benamar, M.M. Bennouna, Geometrically non-linear free vibrations of clamped–clamped beams with an edge crack, *Computers & Structures* 84 (2006) 485–502.
[4] B. Binici, Vibration of beams with multiple open cracks subjected to axial force, *Journal of Sound and Vibration* 287 (2005) 277–295.
[5] H.P. Lin, S.C. Chang, J.D. Wu, Beam vibrations with an arbitrary number of cracks, *Journal of Sound and Vibration* 258 (2002) 987–999.
[6] S. Loutridis, E. Douka, L.J. Hadjileontiadis, Forced vibration behaviour and crack detection of cracked beams using instantaneous frequency, *NDT&E International* 38 (2005) 411–419.
[7] N.T. Khiem, T.V. Lien, The dynamic stiffness matrix method in forced vibration analysis of multiple-cracked beam, *Journal of Sound and Vibration* 254 (2002) 541–555.
[8] C.Y. Wang, C.M. Wang, T.M. Aung, Buckling of a weakened column, *Journal of Engineering Mechanics ACSE* 130 (2004) 1373–1376.
[9] M. Abu-Hilal, Dynamic response of a double Bernoulli–Euler beam due to a moving constant load, *Journal of Sound and Vibration* 297 (2006) 477–491.
[10] T. Kocatürk, M. Şimşek, Vibration of viscoelastic beams subjected to an eccentric compressive force and a concentrated moving harmonic force, *Journal of Sound and Vibration* 291 (2006) 302–322.
[11] H.S. Zibdeh, Stochastic vibration of an elastic beam due to random moving loads and deterministic axial forces, *Engineering Structures* 17 (1995) 530–535.
[12] M.A. Mahmoud, Stress intensity factors for single and double edge cracks in a simple beam subject to a moving load, *International Journal of Fracture* 111 (2001) 151–161.
[13] M.A. Mahmoud, M.A. Abou Zaid, Dynamic response of a beam with a crack subject to a moving mass, *Journal of Sound and Vibration* 256 (2002) 591–603.
[14] C. Bilello, L.A. Bergman, Vibration of damaged beams under a moving mass: theory and experimental validation, *Journal of Sound and Vibration* 274 (2004) 567–582.
[15] H.P. Lin, S.C. Chang, Forced responses of cracked cantilever beams subjected to a concentrated moving load, *International Journal of Mechanical Sciences* 48 (2006) 1456–1463.
[16] F. Delale, F. Erdogan, The crack problem for a nonhomogeneous elastic medium, *Journal of Applied Mechanics ASME* 50 (1983) 609–614.
[17] N. Noda, Z.H. Jin, A crack in functionally gradient materials under thermal shock, *Archives of Applied Mechanics* 64 (1994) 99–110.
[18] Z.H. Jin, R.C. Batra, Some basic fracture mechanics concepts in functionally graded materials, *Journal of Mechanics and Physics of Solids* 44 (1996) 1221–1235.
[19] F. Erdogan, B.H. Wu, The surface crack problem for a plate with functionally graded properties, *Journal of Applied Mechanics ASME* 64 (1997) 448–456.
[20] B.L. Wang, N. Noda, Thermally induced fracture of a smart functionally graded composite structure, *Theoretical and Applied Fracture Mechanics* 35 (2001) 93–109.
[21] G.N. Praveen, J.N. Reddy, Nonlinear transient thermoelastic analysis of functionally graded ceramic-metal plates, *International Journal of Solids and Structures* 35 (1998) 4457–4476.
[22] J. Yang, H.S. Shen, Dynamic response of initially stressed functionally graded rectangular plates resting on elastic foundations, *Composite Structures* 54 (2001) 497–508.
[23] J. Yang, H.S. Shen, Free vibration and parametric resonance of shear deformable functionally graded cylindrical panels, *Journal of Sound and Vibration* 261 (2003) 871–893.
[24] J. Yang, S. Kitipornchai, K.M. Liew, Large amplitude vibration of thermo-electro-mechanically stressed FGM laminated plates, *Computer Methods in Applied Mechanics and Engineering* 192 (2003) 3861–3885.
[25] J. Yang, K.M. Liew, S. Kitipornchai, Dynamic stability of laminated FGM plates based on higher-order shear deformation theory, *Computational Mechanics* 33 (2004) 305–315.
[26] X.L. Huang, H.S. Shen, Nonlinear vibration and dynamic response of functionally graded plates in thermal environments, *International Journal of Solids and Structures* 41 (2004) 2403–2427.
[27] N. Sundaraja, T. Prakash, M. Ganapathi, Nonlinear free flexural vibration of functionally graded rectangular and skew plates under thermal environments, *Finite Element Analysis and Design* 42 (2005) 152–168.
[28] R. Sridhar, A. Chakraborty, S. Gopalakrishnan, Wave propagation analysis in anisotropic and inhomogeneous uncracked and cracked structures using pseudospectral finite element method, *International Journal of Solids and Structures* 43 (2006) 4997–5031.
[29] J. Yang, Y. Chen, Free vibration and buckling analyses of functionally graded beams with edge cracks, *Composite Structures*, doi:10.1016/j.compstruct.2007.03.006.
[30] D. Broek, *Elementary Engineering Fracture Mechanics*, Martinus Nijhoff Publishers, Dordrecht, 1986.